Available online at www.sciencedirect.com
ScienceDirect
Tribology International 41 (2008) 524–534
TRIBOLOGY INTERNATIONAL
www.elsevier.com/locate/triboint

Generalized capstan problem: Bending rigidity, nonlinear friction, and extensibility effect

Jae Ho Jung[a], Ning Pan[a], Tae Jin Kang[b,*]

[a]Division of Textile and Clothing, Department of Biological System Engineering, University of California, Davis, CA 95616, USA
[b]School of MSE, College of Engineering, Seoul National University, Seoul 151-744, South Korea

Received 18 September 2006; received in revised form 1 November 2007; accepted 3 November 2007

Abstract

A theoretical model of the *capstan* problem including the extensibility and the Poisson's ratio of the rod is established in this study. Several cases were examined to investigate the effects of important parameters on the tension transmission efficiency. As a result, the rod extensibility turned out to enhance the tension ratio, competing with the effects of rod bending rigidity and the frictional behaviors of the system. In case of no frictional modification ($n = 1$, the simple Amonton's law), larger initial strain renders greater tension ratio. This effect becomes more remarkable at high radius ratio. However, the effect of the modified frictional law may oppress the effect of rod extensibility if the initial tension T_0 grows larger. The effect of Poisson's ratio also tends to increase the tension ratio. But the amount was almost negligible since the maximum decrease was at most 7.8%. We also calculated the average strain throughout the rod by solving the governing equation and iterating the value of λ_{avg}. Calculated strain throughout the rod was up to 2.6 times larger than initial strain. But this contribution leaded to at most 1.078 times larger radius ratio than the initial rod radius. Thus, it is well enough to consider only the extensibility effect on the increase of the tension ratio. We also presented several prerequisites to establish the model. Three major concerns about this model were introduced and clarified.

Keywords: Capstan equation; Extensibility; Poisson's ratio; Tension transmission; Power–law friction; Bending rigidity

1. Introduction

A tensioned rod, rope, fiber, or film wound over a circular shaped body is frequently seen in many mechanical set ups and applications. A well-known and widely used relationship is the so-called *capstan* equation [1], or Euler's equation of tension transmission. In general, the word "capstan" has the following common meanings: a rotating machine which is used to control ropes that are wound around it and used to pull/release a ship, or a rotating spindle used to move recording tape through the mechanism of a tape recorder. But the usage of the term "capstan equation" is not confined within the above two cases. In pure mechanical viewpoint, a capstan is a typical example of the physical equilibrium accompanying friction between rope or film-like solid and circular shaped body. So the capstan equation is widely used to analyze the mechanical behavior of the film/rope-like solid in contact with circular profiled surface. Rope rescue system [2,3] is a good example for applying capstan equation to their mechanical analysis. In textile area, capstan equation has been a basic equation to analyze its process. Several papers [4–8] using the capstan equation were introduced in tribological area.

Although they are significant contributions up to nowadays, all these papers are based on so called "classical capstan equation" and it should be noted that the modification of capstan equation itself is seldom introduced nor applied in the area of tribology. While it is commonly introduced and derived to help understand the mathematical procedure in all the previously refered papers, the classical capstan equation is the most simplified relationship one can derive between the incoming and outgoing tensions in the rods because it is based on the force equilibrium under such ideal condition as complete

*Corresponding author.
E-mail addresses: jaejung@snu.ac.kr (J.H. Jung), npan@ucdavis.edu (N. Pan), taekang@snu.ac.kr (T.J. Kang).

0301-679X/$ - see front matter © 2007 Elsevier Ltd. All rights reserved.
doi:10.1016/j.triboint.2007.11.005

Nomenclature

r_1	radius of the rod before extension	ε	normal strain of the infinitesimal element of the rod
r_1'	radius of the rod after extension	v	Poisson's ratio of the rod
r_2	radius of the circular shaped body	T	tension force
R	total radius, r_1+r_2	T_0	incoming/initial tension force
ρ	the radius ratio between rod and body, r_2/r_1	T_1	outgoing/result tension force
φ	contact angle from the start point to arbitrary point before extension	τ_A	apparent tension ratio between T_1 and T_0
φ'	contact angle from the start point to arbitrary point after extension	τ_C	actual tension ratio, $T(\theta)/T(0)$
ω_0	inclined angle of incoming tension T_0	Q	shear force
ω_1	inclined angle of outgoing tension T_1	N	normal force
θ	total contact angle	F_μ	frictional force
		M	bending moment
		E	Young's modulus of the rod
		A	cross-sectional area of the rod

close contact with no extension, flexible rod with no bending rigidity, and no frictional modification. Therefore many engineers have found that this classical *capstan* equation does not hold well for actual cases—some attempts have been made to compensate these shortcomings: Taking the bending rigidity into account [9,13–16] is the first act, whereas taking the nonlinear frictional relationship into account [11,12,16] is another one. Since the bending rigidity of the rod considered means the resistance of the rod to be bent around the drum, exerted tension is less transmitted in the presence of rod bending rigidity. In addition, the rod rigidity renders the direction of the exerted tension to be inclined inside the drum. Meanwhile, the nonlinear frictional behavior considered expresses the formula of the frictional law as power–law relationship, not linear one. Since the exponent in the formula is less than unity, it reflects the decrease of the frictional coefficient with the increase of the exerted tension.

As the most recent summary and revision of the previous attempts resolving all the previous shortcoming including Howell's contradiction (see Ref. [16]), Jung et al. [16] combined these two major corrections into one, and concluded that both factors tend to decrease the tension transmission ratio—the nonlinear frictional behavior is much more dominant than the bending rigidity. However, the initial tension should be sufficiently large so that this tension ratio decrease may actually appear.

Another important factors, but never considered before, are the extensibility and Poisson's ratio of the rod due to tension. Their effects can be very important in flexible rod such as wires or ropes. It should be noted that no published work has been made available to deal with both the extensibility and the Poisson's effects of the rod, let alone to combine them with the bending rigidity and power–law friction into a complete capstan problem solution. In most related reports, the elongation and the associated lateral contraction of the tension member were simply ignored, which in many cases, turned out to be significant negligence. Therefore, the purpose of this research is to establish a more generalized theory including such factors as extension and Poisson's ratio, in addition to the bending rigidity and power–law friction, so as to examine the extent of their influences. This work will be also useful to those who are to identify which is positive and which is not among the following factors: the extension of the rod and the decrease in the diameter due to the applied tension versus the rod bending rigidity and nonlinear frictional behavior.

2. Theoretical approach

2.1. Prerequisites before deriving governing equation

2.1.1. Direction of frictional force and contact angle measurement

Before deriving the governing equation, there exist some prerequisites we must clarify. First assigning the incoming and outgoing tensions in a rod as T_0 or T_1—Fig. 1 shows the typical situation of the bent elastic rod in contact with the capstan.

Because of the rod bending rigidity, the tension T_0 or T_1 at the both ends of the rod are no longer in the tangent direction: it splits into two components, the normal force $Q(\theta)$ bending the rod to maintain the contact with the capstan and the tangent force $T(\theta)$ pulling the rod. There exist tangential and normal components of the incoming tension as:

$$T_1^2 = T(\theta)^2 + Q(\theta)^2, \quad T(\theta) = T_1 \cos\omega_1, \quad Q(\theta) = T_1 \sin\omega_1$$

Similarly at the other end, there exist tangential and normal components of the outgoing tension as

$$T_0^2 = T(0)^2 + Q(0)^2, \quad T(0) = T_0 \cos\omega_0, \quad Q(0) = T_0 \sin\omega_0$$

An interesting feature in the above figure is that there is no definite answer which is bigger between $T(0)$ and $T(\theta)$. The key lies in the directions of the frictional force. If the frictional force goes toward $T(0)$, $T(\theta)$ is larger than $T(0)$. And consequently the contact angle is measured counter

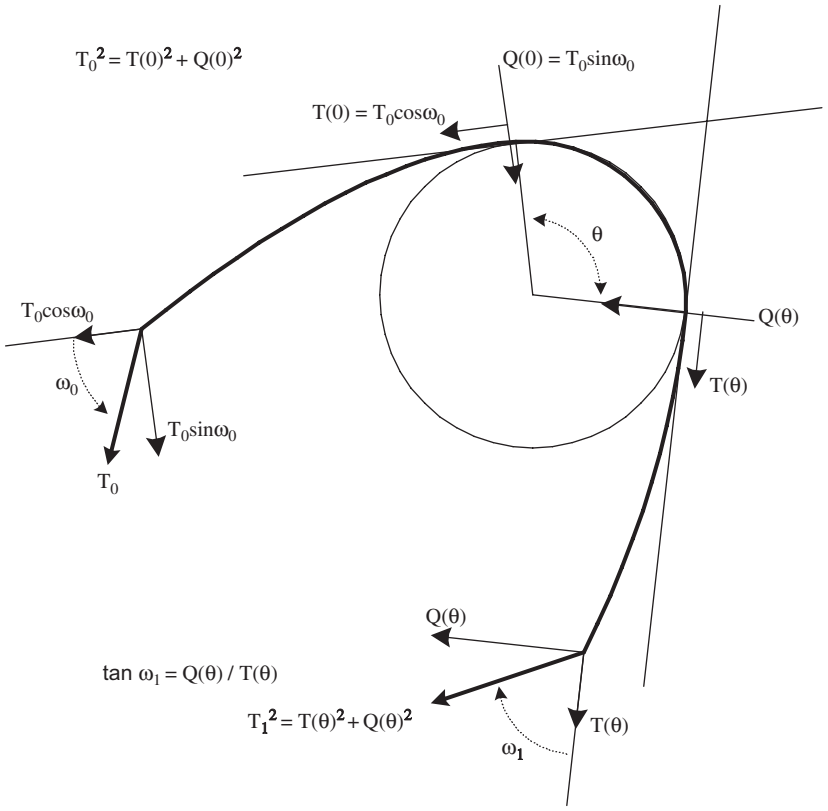

Fig. 1. Typical situation of bent elastic rod in contact with circular body.

clockwise: starting as zero from $T = T_0 \cos\omega_0$ to θ at $T = T_1 \cos\omega_1$.

Otherwise, the reverse is true and the contact angle is measured clockwise. This feature should be considered during drawing the free body diagram. Another interesting but confusable issue is that there exist two opposite ways of measuring the contact angle—clockwise and counter clockwise directions. According to the clockwise measurement, the contact angle is put as zero at $T = T_0 \cos\omega_0$, and as θ at $T = T_1 \cos\omega_1$ while it is put as zero at $T = T_1 \cos\omega_1$, and θ at $T = T_0 \cos\omega_0$ according to the counter clockwise measurement. Figs. 2a and b illustrate the situations. In these figures, φ and γ denotes the intermediate contact angle measured clockwise and counter clockwise. Apparently, the following relationships are satisfied:

$$\varphi + \xi = \theta, \quad d\varphi = -d\xi, \quad T(\varphi) \rightleftarrows T(\theta - \xi) \tag{1.1}$$

Note that by using Eq. (1.1), the tension with counter clockwise measurement can be transformed into the tension with clockwise one. Here are two examples of transformation.

In case of an inextensible funicular rod, the above equation leads to the following well-known classical capstan equation:

$$T(\varphi) = T_0 e^{\mu\varphi}, \quad T(\gamma) = T_1 e^{-\mu\gamma}, \tag{1.2}$$

$$T(\theta - \gamma) = T_1 e^{-\mu(\theta-\gamma)} = T_1 e^{-\mu\theta} e^{\mu\gamma}, \tag{1.3}$$

$$\therefore T_1 = T_0 e^{\mu\theta}.$$

In the existence of rod rigidity, it leads to the following:

$$T(\varphi) = C_1 e^{\alpha\varphi} + C_2 e^{\beta\varphi}, \quad T(\gamma) = C_1' e^{-\alpha\gamma} + C_2' e^{-\beta\gamma}, \tag{1.4}$$

$$T(\theta - \gamma) = C_1' e^{-\alpha(\theta-\gamma)} + C_2' e^{-\beta(\theta-\gamma)} = C_1' e^{-\alpha\theta} e^{\alpha\gamma} + C_2' e^{-\beta\theta} e^{\beta\gamma}, \tag{1.5}$$

$$\therefore C_1' = C_1 e^{\alpha\theta}, \quad C_2' = C_2 e^{\beta\theta},$$

where α and β are appropriate constants depending on the frictional coefficient and the radii of rod and contact body. From now on we only use the clockwise measurement of the contact angle so that $T(\theta) = T_1 \cos\omega_1$ is always greater than $T(0) = T_0 \cos\omega_0$.

2.1.2. Initial and boundary conditions

Next, it is necessary to find and clarify the initial and boundary conditions. From Fig. 1, it is clear that

$$T(0) = T_0 \cos\omega_0, \quad Q(0) = T_0 \sin\omega_0,$$

$$T_0 = \sqrt{\{T(0)\}^2 + \{Q(0)\}^2} \tag{1.6}$$

$$T_1 = \sqrt{\{T(\theta)\}^2 + \{Q(\theta)\}^2}, \quad \tan\omega_1 = \frac{Q(\theta)}{T(\theta)}. \tag{1.7}$$

Apparently, the inclined angle ω_0 and ω_1 will be zero in case of no bending rigidity. On the other hand, these angles are essential for a rod with bending rigidity to make an equilibrium shape [5]. In other words, the existence of rod

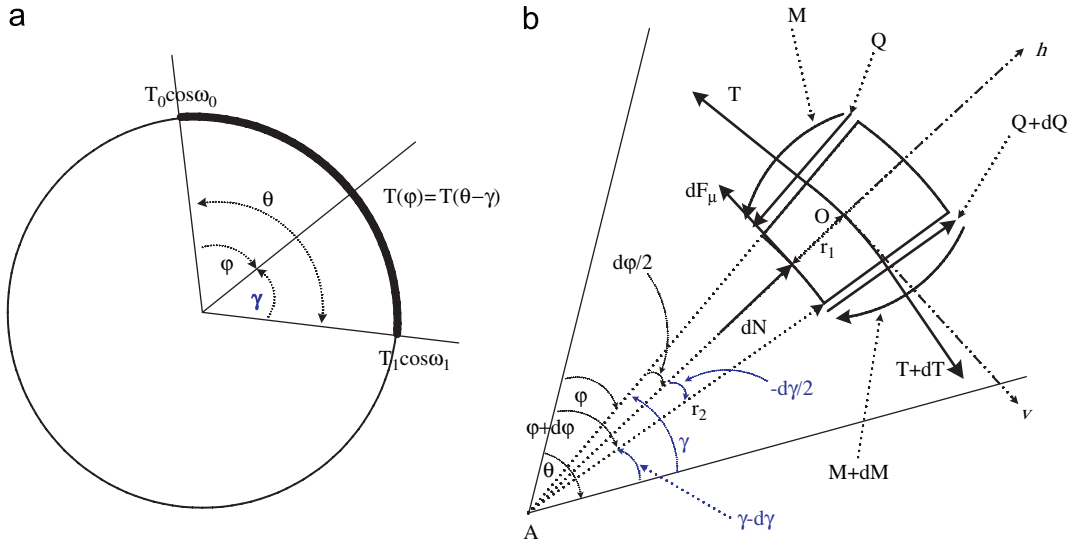

Fig. 2. Two possible ways counting the contact angle—(a) the whole contact region, (b) on the free body diagram.

rigidity affects both the shape of the rod in the deflected region and the actual tension ratio $T(\theta)/T(0)$ in the contact region.

2.1.3. Expression of tension ratio

As mentioned above, the apparent tension ratio T_1/T_0 becomes different from the actual tension ratio $T(\theta)/T(0)$ because of the existence of inclined angle of load ω_0 and ω_1. To distinguish them from each other, we define two different tension ratios—apparent tension ratio (τ_A), and actual tension ratio (τ_C), respectively, as

$$\tau_A = \frac{T_1}{T_0} = \sqrt{\frac{\{T(\theta)\}^2 + \{Q(\theta)\}^2}{\{T(0)\}^2 + \{Q(0)\}^2}}, \quad \tau_C = \frac{T(\theta)}{T(0)}, \tag{1.8}$$

From the above equation, one can see that the apparent tension ratio reflects the effect of shear forces $Q(0)$ and $Q(\theta)$ as well. Only in case of inextensible funicular rod—no shear force, no bending moment—will the apparent tension ratio become equal to the actual ratio. If a rod has bending rigidity, there will be shear force and the inclined angles ω_0 and ω_1.

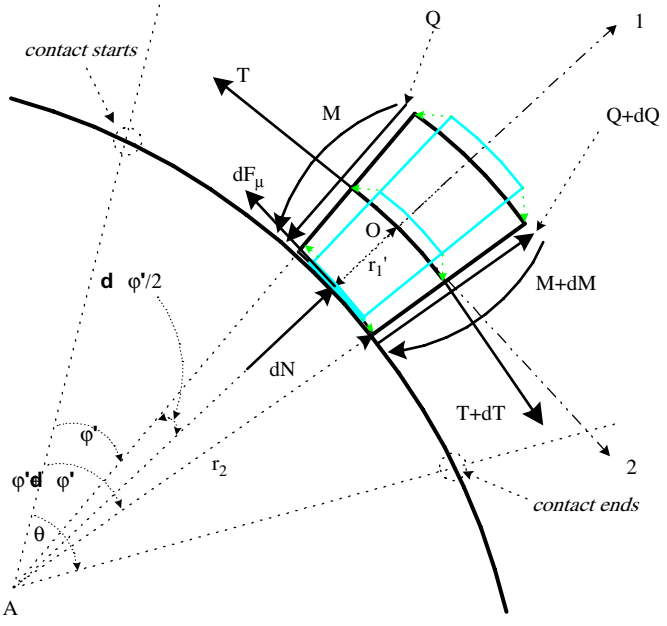

Fig. 3. The free body diagram of the infinitesimal element of extended rod in equilibrium of force and moment and its boundary at the circular contact region.

2.2. Derivation of governing equations upon rod extension

Fig. 3 shows the free body diagram of a rod wound over a capstan. It also shows how the extension of the neutral line renders the infinitesimal length of the rod to increase from dl to dl'. Manipulating it mathematically leads to the following relationship:

$$dl' = (1+\varepsilon)\,dl, \tag{2.1}$$

$$dl = (r_1 + r_2)\,d\varphi, \quad dl' = (r_1' + r_2)\,d\varphi' \tag{2.2}$$

where all the primes indicate the parameters after extension. Here, we define the normal strain, ε, as

$$\varepsilon = \frac{T\cos(d\varphi/2) - Q\sin(d\varphi/2) + dF_\mu}{EA} \approx \frac{T - (Q/2)\,d\varphi + dF_\mu}{EA}, \tag{2.3}$$

2.2.1. Normal strain and radius of the rod in contact region upon extension

Fig. 3 presents the free body diagram of the infinitesimal element of extended rod in equilibrium of force and moment and its boundary at the circular contact region.

2.2.2. Poisson's effect

In the present work, we assume uniform Poisson's effect—uniform radius of the rod after extension. Thus, the radius of the rod after extension becomes

$$r_1' = r_1(1 - v\hat{\varepsilon}), \quad \hat{\varepsilon} = \lambda\varepsilon_0, \quad \varepsilon_0 = \frac{T_0}{EA}, \tag{2.4}$$

where ε_0 is the initial strain, and $\hat{\varepsilon}$ is the effective or average strain throughout the whole range of contact. So the key to include the Poisson's effect in the model lies in the determination of the parameter λ connecting the initial and effective strains. If we assume that the Poisson effect depends upon the inclined angle and the incoming strain, we can have $\lambda = \cos\omega_0$ as the simplest choice. This value is equivalent to the strain at $T(0) = T_0\cos\omega_0$. This choice actually represents the minimum Poisson effect.

The second but more reasonable choice is to guess the effect acts on the rod constantly with the amount of average strain throughout the rod. According to this choice, the expression of the parameter λ leads to the following:

$$\hat{\varepsilon} = \frac{\int_0^\theta \varepsilon\,\mathrm{d}\varphi}{\int_0^\theta \mathrm{d}\varphi} = \frac{1}{\theta}\int_0^\theta \frac{T}{EA}\,\mathrm{d}\varphi = \frac{\varepsilon_0}{\theta}\int_0^\theta \overline{T}\,\mathrm{d}\varphi \tag{2.5}$$

$$\therefore \lambda = \frac{1}{\theta}\int_0^\theta \overline{T}\,\mathrm{d}\varphi, \quad \overline{T} = \frac{T}{T_0} \tag{2.6}$$

where $\bar{T}$ is the normalized tension. Existing difficulty in using the above relationship is that we need to solve the derived governing equation prior to determining the value of λ. Since λ is involved with $\bar{T}$ in Eq. (2.6), we should guess the value of λ first and solve the governing equation to obtain the data of $\bar{T}$. Next we should iterate the value of λ until Eq. (2.6) is satisfied. This procedure renders the derived governing equation to be implicit. In case of large change of rod radius, the second choice is desired since it is more realistic. However, it is meaningful to carry out the modeling according to both the former and latter choice and figure out how much the error level will be by avoiding complexity. It helps us find the acceptable range of radius ratio to adopt the first choice with maintaining the desired accuracy. Anyway, substituting Eqs. (2.2)–(2.6) into (2.1) and eliminating all the higher order terms give

$$\mathrm{d}\varphi' = \frac{(1+\varepsilon_0\overline{T})(r_1+r_2)}{\{r_1(1-v\lambda\varepsilon_0)+r_2\}}\,\mathrm{d}\varphi = \kappa(1+\varepsilon_0\overline{T})\,\mathrm{d}\varphi,$$
$$\kappa = \frac{1+\rho}{(1-v\lambda\varepsilon_0)+\rho}, \tag{2.7}$$

where κ is a parameter reflecting the extensibility. The above relationships are used to derive the governing equation in next session.

2.2.3. Equilibrium equations in the contact region and frictional properties

From the force balance along the 1, 2 directions and the moment equilibrium at point "O" in Fig. 3, we can obtain three following differential equations:

$$\mathrm{d}T + Q\,\mathrm{d}\varphi' - \mathrm{d}F_\mu = 0, \tag{2.8}$$

$$\mathrm{d}Q - T\,\mathrm{d}\varphi' + \mathrm{d}N = 0, \tag{2.9}$$

$$\mathrm{d}M - Q(r_1' + r_2)\,\mathrm{d}\varphi' + r_1'\,\mathrm{d}F_\mu = 0. \tag{2.10}$$

Also, all the existent contacts are regarded as continuous. As for frictional properties, the classical Amonton's law of friction states that the frictional force F_μ is proportional to the normal force N. However, it is well known that this law does not hold true in several kinds of materials—especially in polymeric and textile materials. An improved relationship between the frictional and normal force is the following:

$$F_\mu = \alpha N^n, \quad n \leqslant 1 \tag{2.11}$$

where α and n are material constants. Note that the above relationship does not contain the radius of the rod or wheel, while Howell's notation does. It is very important. Calculated frictional coefficient should not vary with the change of the rod/wheel radius.

However, taking Howell's notation [11,16] renders the calculated frictional coefficient larger than unity as the radius of the wheel grows larger (see Ref. [16] for more detailed explanation). When the value of n goes to unity, this becomes the classical Amonton's law. Many polymeric materials take the value $n = 0.67$ [11].

2.2.4. Governing equations

Bearing in mind that the rod is an elastic solid ($\mathrm{d}M = 0$), we can obtain the following equation from Eqs. (2.8)–(2.11):

$$\frac{\mathrm{d}^2T}{\mathrm{d}\varphi'^2} + \frac{1}{n}\frac{\rho}{(1-v\lambda\varepsilon_0)}\left(\frac{1-v\lambda\varepsilon_0+\rho}{\alpha\rho}\right)^{1/n} \times T^{(1-n)/n}\frac{\mathrm{d}T}{\mathrm{d}\varphi'} - \frac{\rho}{(1-v\lambda\varepsilon_0)}T = 0 \tag{2.12}$$

Substituting Eq. (2.8) into (2.13) gives the following:

$$\frac{\mathrm{d}^2\overline{T}}{\mathrm{d}\varphi^2} + \frac{\rho\kappa((1-v\lambda\varepsilon_0+\rho)/(\alpha\rho))^{1/n}T_0^{(1-n)/n}}{n(1-v\lambda\varepsilon_0)} \times \overline{T}^{(1-n)/n}(1+\varepsilon_0\overline{T})\frac{\mathrm{d}\overline{T}}{\mathrm{d}\varphi} - \frac{\kappa\varepsilon_0}{1+\varepsilon_0\overline{T}}\left(\frac{\mathrm{d}\overline{T}}{\mathrm{d}\varphi}\right)^2 - \frac{\rho\kappa^2(1+\varepsilon_0\overline{T})^2}{(1-v\lambda\varepsilon_0)}\overline{T} = 0 \tag{2.13}$$

$$Q = \frac{T_0(1-v\lambda\varepsilon_0+\rho)(1-v\lambda\varepsilon_0)}{\rho(1+\rho)(1+\varepsilon_0\overline{T})}\frac{\mathrm{d}\overline{T}}{\mathrm{d}\varphi},$$
$$\mathrm{d}F_\mu = \frac{T_0(1-v\lambda\varepsilon_0+\rho)}{\rho}\,\mathrm{d}\overline{T}, \quad N = \left(\frac{F_\mu}{\alpha}\right)^{1/n},$$
$$M = \frac{EI}{R}, \quad \kappa = \frac{1+\rho}{1-v\lambda\varepsilon_0+\rho}. \tag{2.14}$$

Eq. (2.13) together with Eq. (2.14) is the normalized governing equation for calculating tension ratio with extension and frictional drop. Note that the initial tension T_0 in

Eq. (2.13) can only be eliminated in case of the classical Amonton's law of friction. In other words, the tension ratio in fact depends upon the initial tension in general. Since the equation cannot be solved analytically, numerical procedure, the fourth-order Runge–Kutta method, is chosen here. Eq. (2.13) can be divided into the following two compatible first-order ODEs:

$$\frac{d\overline{T}(\varphi)}{d\varphi} = \overline{U}(\varphi), \tag{2.15}$$

$$\begin{aligned}\frac{d\overline{U}(\varphi)}{d\varphi} = & -\frac{\rho(1+\rho)((1-\nu\lambda\varepsilon_0+\rho)/\alpha\rho)^{1/n}T_0^{((1-n)/n)}}{n(1-\nu\lambda\varepsilon_0)(1-\nu\lambda\varepsilon_0+\rho)} \\ & \times\{\overline{T}(\varphi)\}^{((1-n)/n)}\{1+\varepsilon_0\overline{T}(\varphi)\}\overline{U}(\varphi) \\ & +\frac{1+\rho}{1-\nu\lambda\varepsilon_0+\rho}\frac{\varepsilon_0}{1+\varepsilon_0\overline{T}(\varphi)}\{\overline{U}(\varphi)\}^2 \\ & +\frac{(1+\rho)^2}{(1-\nu\lambda\varepsilon_0+\rho)^2}\frac{\rho\{1+\varepsilon_0\overline{T}(\varphi)\}^2}{(1-\nu\lambda\varepsilon_0)}\overline{T}(\varphi).\end{aligned} \tag{2.16}$$

To solve these differential equations, we also need two equivalent boundary conditions as below:

$$\overline{T}(0)=\cos\omega_0, \quad \overline{U}(0)=\frac{\rho(1+\rho)(1+\varepsilon_0\cos\omega_0)}{(1-\nu\lambda\varepsilon_0+\rho)(1-\nu\lambda\varepsilon_0)}\sin\omega_0. \tag{2.17}$$

As mentioned before, the choice of the expression for the parameter λ will be the following:

$$\lambda_{\min}=\cos\omega_0 \tag{2.18a}$$

$$\lambda_{\text{avg}}=\frac{1}{\theta}\int_0^{\theta}\overline{T}\,d\varphi. \tag{2.18b}$$

If we choose the expression of the parameter $\lambda=\lambda_{\min}$, there is no iteration needed in solving Eqs. (2.15) and (2.16). All processes will be explicit. On the other hand, we can estimate the value of λ at first and iterate it until Eq. (2.18b) is satisfied and then we have $\lambda=\lambda_{\text{avg}}$. In case of zero Poisson's effect, λ vanishes. Specific comparisons between the two choices will be provided in next section.

3. Results and discussions

In this section, we will calculate the apparent and actual tension ratios with two major categories: with extensibility effect only, and with both extensibility and Poison's effects. Each category includes the classic and modified frictional laws cases, respectively. Table 1 provides the materials properties used in the predictions.

3.1. Tension ratio with extensibility only

Case 1.1. With extensibility and classic frictional law ($n=1$, $\alpha=0.4$) under zero Poisson's effect ($\nu=0$)–$\omega_0=20^\circ$ with different radius ratios $\rho=5$, and 50 at three initial strain levels $\varepsilon_0=0$ (no extension), 0.05, 0.1.

The above case is chosen to investigate the effect of extensibility and rod rigidity only. We calculate the apparent and actual tension ratios from Eqs. (2.13) and (2.14) and compare the results with those from the classical capstan equation as shown in Fig. 4 as against the contact angle θ.

Apparently at a given contact angle, the tension ratio increases with the increase of the initial strain ε_0. Another interesting feature is that the actual tension ratio τ_C is always greater than the apparent tension ratio τ_A. On the other hand, the tension ratios with zero extension are smaller than that in case of the classical capstan equation on the whole due to the effect of rod rigidity, as reported in our previous work [15]. Smaller radius ratio renders more tension ratio drop, but the existence of the inclined angle ω_0 competes with it.

It is also interesting that the actual tension ratio in Fig. 4b takes larger value than the classical capstan equation at first, while it becomes smaller around the range of $\theta\approx80^\circ$. Though not presented, calculated value of inclined angle ω_1 rapidly converges to certain level as the contact angle grows larger, while the effect of rod rigidity gradually appears as the contact angle grows. Thus, the effect of inclined angle is more dominant at relatively low contact angle, while the effect of rod rigidity (or radius ratio) becomes more dominant at high contact angle. So the tension ratios show partially greater tendency at initial small contact angle, especially for the actual tension ratio τ_C in Fig. 4b, while this tendency is reversed at high contact angle.

Fig. 5 shows the same apparent and actual tension ratio versus contact angle θ and the only change is the increase of radius ratio ρ from 5 to 50. However, this change alone is enough to significantly increase the tension ratios compared with the data in Figs. 4a and b. The effect of extensibility is so remarkable that even apparent tension ratios in Fig. 5a are always greater than that by the classical capstan equation. The maximum increase of the apparent and actual tension ratio is 40.5% and 49.6% compared with the data from the classical capstan equation, respectively.

Another interesting feature is that even the apparent and actual tension ratios in Figs. 5a and b with no extension are

Table 1
Material properties for Case 1

Rod radius, r_1 (mm)	Rod modulus, E (MPa)		Frictional factor, α	Power–law exponent, n		Inclined angle, ω_0 (°)	Poisson's ratio, ν		Radius ratio, ρ		Initial strain, ε_0		
1.0	10.0	1.0	0.4	1	0.67	20	0	0.3	5	50	0	0.05	0.1

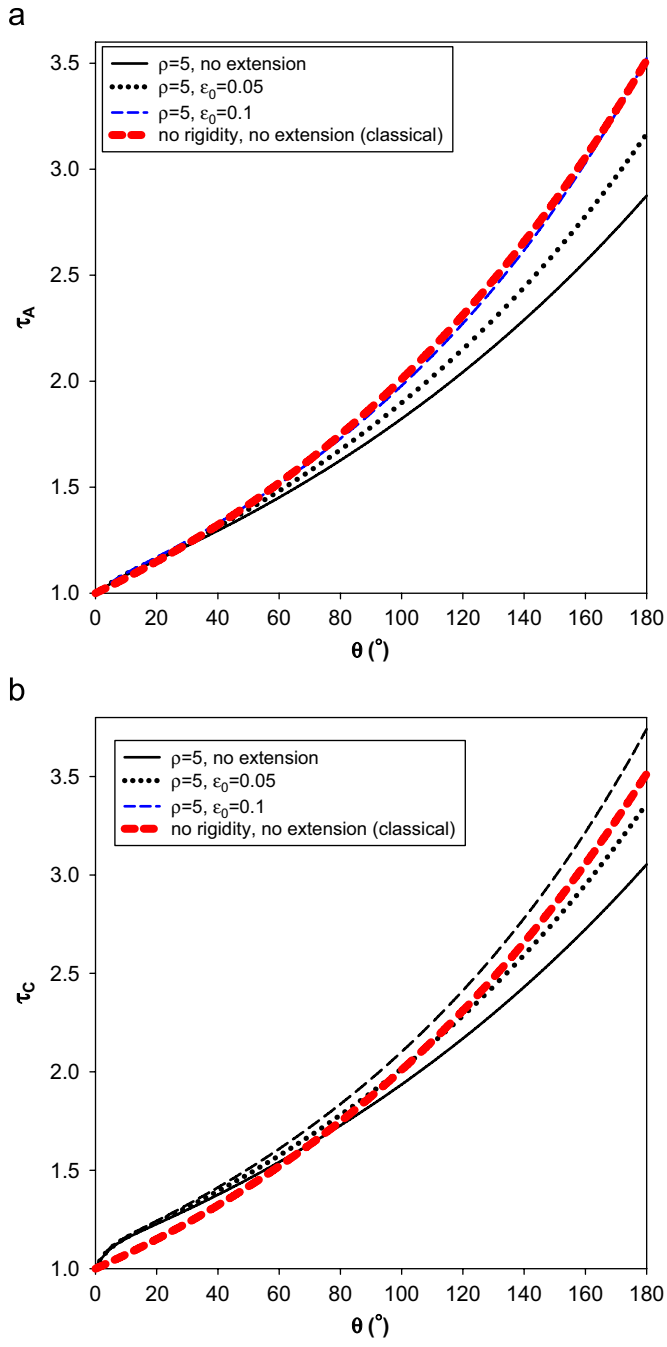

Fig. 4. (a) Comparison of the apparent tension ratio τ_A versus contact angle θ in case of $\rho = 5$ at different initial strains. (b) Comparison of the actual tension ratio τ_C versus contact angle θ in case of $\rho = 5$ at different initial strains.

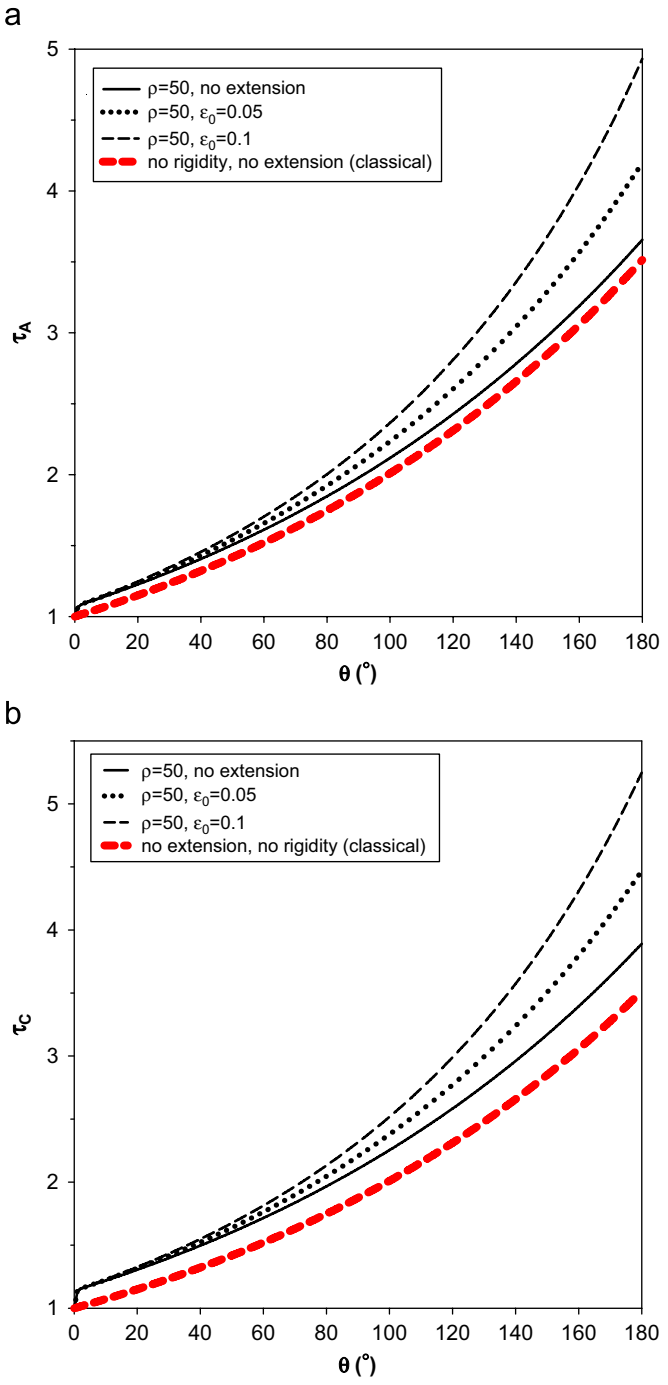

Fig. 5. (a) Comparison of the apparent tension ratio τ_A versus contact angle θ in case of $\rho = 50$ at different initial strains. (b) Comparison of the actual tension ratio τ_C versus contact angle θ in case of $\rho = 50$ at different initial strains.

also greater than the tension ratio in the classical capstan equation. It results from the role of the inclined angle ω_0 and its existence enhances the tension ratios. It has been shown in our previous work [15] that the actual and apparent tension ratio is always smaller than the tension ratio of the classical capstan equation if $\omega_0 = 0$. Of course these increases will be more remarkable if the inclined angle ω_0 grows larger. Thus, it can be concluded that the extensibility of the rod enhances the tension ratio, and this effect becomes more dominant as the radius ratio or the inclined angle ω_0 increases.

Next, we are to investigate the dependence of the tension ratios on the frictional behaviors. Note that the tension ratios in this case are affected by the initial tension T_0, and our previous work [16] reported that the increase of the initial tension T_0 decreases the tension ratio due to the nonlinearity of the frictional law. Since T_0 depends upon the modulus of the rod, it is necessary to compare the

tension ratio with different choices of $E = 1$ and 10 MPa, respectively. All the other parameters are the same as:

Case 1.2. Extensibility effect with frictional modification under zero Poisson's ratio: $-n = 0.67$, $\alpha = 0.4$, $v = 0$, $\omega_0 = 20^\circ$, $\varepsilon_0 = 0$, 0.05, 0.1, $E = 1.0$, 10 MPa, $\rho = 5$, 50.

where calculated initial tension $T_0 = 1.57018$, 3.1415 N for $E = 10$ MPa and 0.15708, 0.31415 N for $E = 1.0$ MPa, respectively. So the tension ratios with no extension are calculated with the same initial tensions.

Figs. 6a and b show the apparent and actual tension ratios versus contact angle θ in case of $\rho = 5$, $E = 10$ MPa at $\omega_0 = 0$, 0.05, 0.1, compared with the data from the classical capstan equation. Unlike the previous data, huge decreases of tension ratios about 40% are observed. The most distinguished feature from the previous case is that the tension ratio depends upon the initial tension. Look at Eq. (2.13). The term T_0 survives and affects the calculated tension ratio. Shown tendency in Fig. 6 tells us that higher initial tension decreases the tension ratio more, which was already reported previously [10]. Since the initial tension T_0 calculated from the data in Case 1.2 is "sufficiently large" enough to show the effect of this modification, calculated tension ratios are greatly decreased. Of course the rod extensibility itself enhances the tension ratio. (Compare solid and dotted line of the same color with each other.) But the increase of ε_0 also caused the increase of the initial tension, which may oppress the extensibility effect. Thus, it caused the decrease of the tension ratio. (Compare two solid lines with each other.)

Figs. 7a and b show the apparent and actual tension ratios versus contact angle θ at $\rho = 5$, $\varepsilon_0 = 0$, 0.05, 0.1, $E = 1.0$ MPa compared with the classical capstan equation. Since the initial tension is decreased up to 1/10 level, the effect of rod rigidity becomes more significant. Thus, the tension ratios decreased less compared with the data in Figs. 6a and b. In addition, the effect of rod extensibility itself is also enhanced with the decrease of the initial tension. (See the solid and dotted line with the same color.) Nevertheless, the tension ratios with $\varepsilon_0 = 0.1$ are still smaller than those with $\varepsilon_0 = 0.05$ since the initial tension is increased from 0.15708 to 0.31415. Of course this feature comes from the effect of frictional modification, not the extensibility effect itself.

Fig. 8 shows the apparent and actual tension ratios versus contact angle θ in case of $\rho = 50$ relative to the classical capstan equation. Since the radius ratio is increased by 10 times, the extensibility effect becomes much more significant, while the effect of frictional nonlinearity still be the same and the effect of rod rigidity grows smaller. Thus, the tension ratios with $\varepsilon_0 = 0.05$ exceed the tension ratio from the classical capstan equations, while the ratios with $\varepsilon_0 = 0.1$ still show smaller tendencies.

In summary, the rod extensibility enhances the tension ratio by competing with the reversing effects of rod rigidity and frictional nonlinearity. For linear friction ($n = 1$),

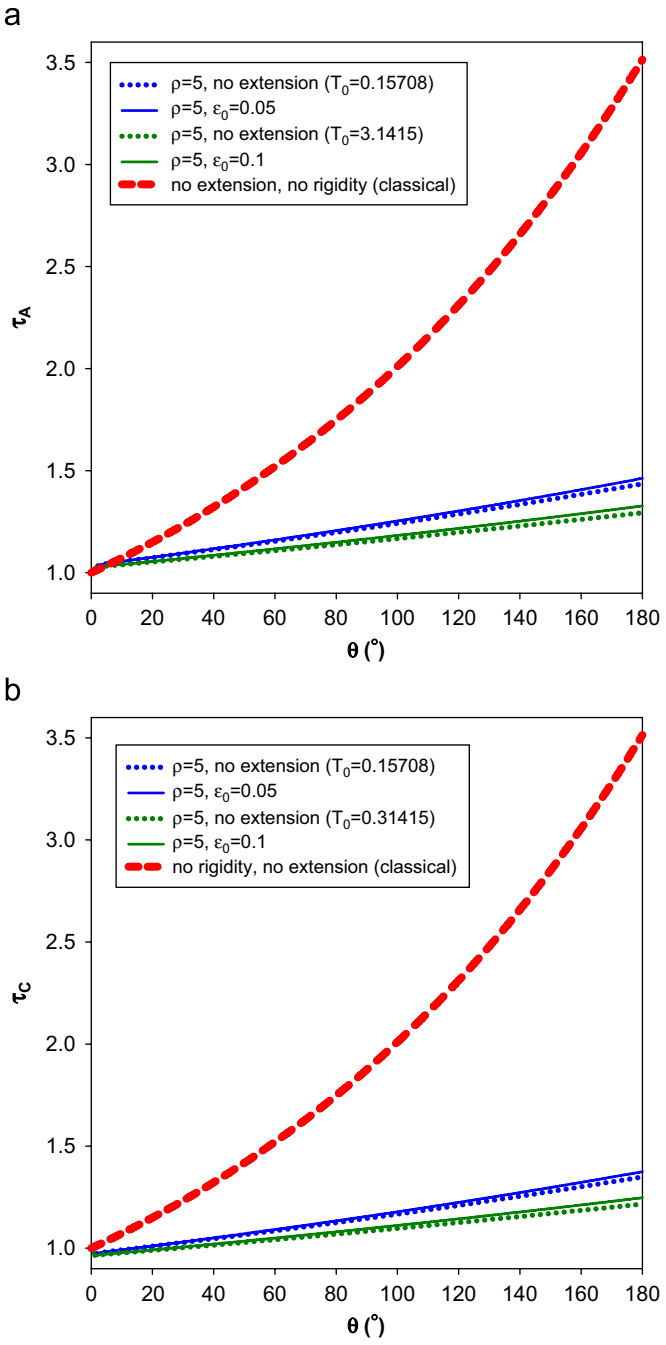

Fig. 6. (a) Comparison of the apparent tension ratio τ_A with nonlinear friction versus contact angle θ for $\rho = 5$, $E = 10$ MPa at different initial strains. (b) Comparison of the actual tension ratio τ_C with nonlinear friction versus contact angle θ for $\rho = 5$, $E = 10$ MPa at different initial strains.

larger initial strain renders more increase of the tension ratio. This effect becomes more remarkable at high radius ratio. However, the effect of the frictional nonlinearity oppresses the effect of rod extensibility if the initial tension T_0 grows larger. In case of frictional nonlinearity ($n = 0.67$), tension ratio with $\varepsilon_0 = 0.1$ is smaller than that with $\varepsilon_0 = 0.05$. This tendency looks opposite to the case of linear friction, and it is caused by the initial tension, not by the rod extensibility since the initial tension is increasing

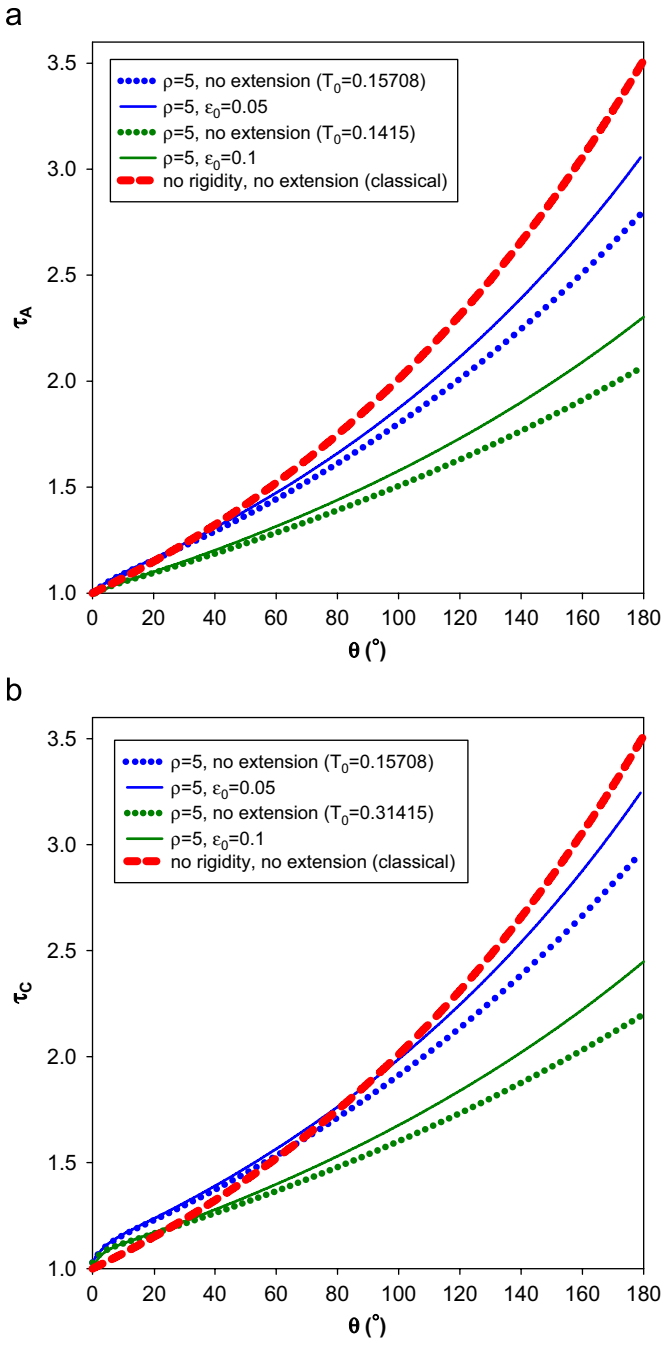

Fig. 7. (a) Comparison of the apparent tension ratio τ_A with frictional nonlinearity versus contact angle θ in case of $\rho = 5$, $E = 1$ MPa at different initial strains. (b) Comparison of the actual tension ratio τ_C with frictional nonlinearity versus contact angle θ in case of $\rho = 5$, $E = 1$ MPa at different initial strains.

with the increase of the initial strain. Therefore, more flexible rod with larger radius of contact wheel enhances the tension ratio at the same level of the initial strain.

3.2. Tension ratios with extensibility and Poisson's effect

In this session, we are to include the Poisson's effect to the calculated tension ratios and investigated their changes. We first calculate $\lambda_{avg}/\lambda_{min}$ with the help of Eqs. (2.15)–(2.17)

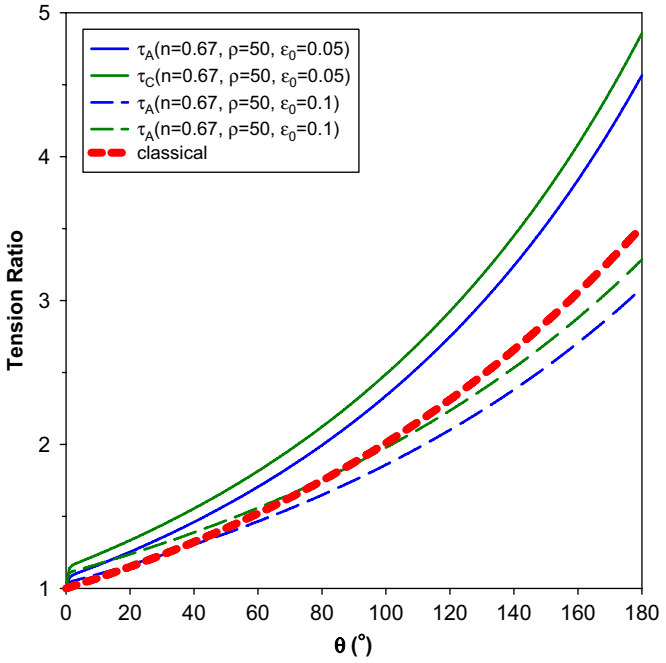

Fig. 8. Comparison of the apparent and actual tension ratios with frictional nonlinearity versus contact angle θ for $\rho = 50$, $E = 1$ MPa at different initial strains.

assuming that the Poisson's ratio is 0.3, as in the most common elastic solids.

Case 2. $n = 1$, $\rho = 5$, $\alpha = 0.4$, $\varepsilon_0 = 0.05$, 0.1, $\omega_0 = 20^\circ$, $v = 0.3$.

Fig. 9 shows $\lambda_{avg}/\lambda_{min}$ versus contact angle θ in case of linear friction ($\alpha = 0.4$, $n = 1$), $\rho = 5$, 50, $\varepsilon_0 = 0.05$, 0.1, $\omega_0 = 20^\circ$ and $v = 0.3$. Apparently, the average strains are larger than the initial strain by up to 2.6 times, and this difference grows larger as the initial strain and/or radius ratio increases. However, the increase of the tension ratio is not so large as expected. Fig. 10 shows the apparent tension ratio versus contact angle θ when $v = 0$ and 0.3, respectively. The maximum increase of the tension ratios is less than 5% in both cases. In fact, Poisson's effect is equivalent to the decrease of the rod radius. From Eq. (2.4), we obtain the following expressions of decreased radius of the rod:

$$\frac{r_1 - r_1'}{r_1} = \frac{\lambda_{avg}}{\lambda_{min}} v\varepsilon_0 \cos \omega_0. \tag{R-1}$$

Calculated percentage of the minimum decrease in rod radius using the above equation is less than 7.3%. It implies that the increase of the radius is at most 7.8%. This difference is negligible even in case of $\rho = 5$ because the increased ratio is $\rho = 5.39$.

Moreover, our previous work reported that the effect of radius ratio diminishes at high value. So the effect of Poisson's ratio also grows smaller. Thus, it is well enough to consider the extensibility effect on the increase of the tension ratio.

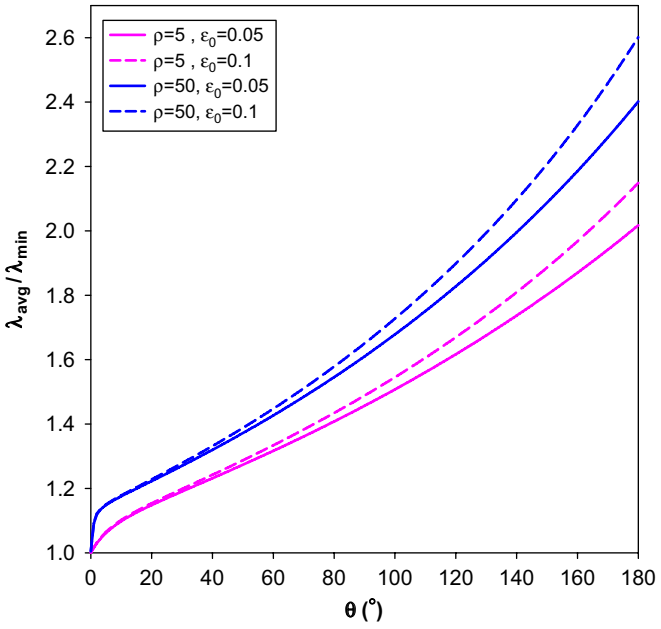

Fig. 9. $\lambda_{avg}/\lambda_{min}$ versus contact angle θ in case of $\alpha = 0.4$, $n = 1$, $\rho = 5$, 50, $\varepsilon_0 = 0.05$, 0.1, $\omega_0 = 20^\circ$ and $v = 0.3$.

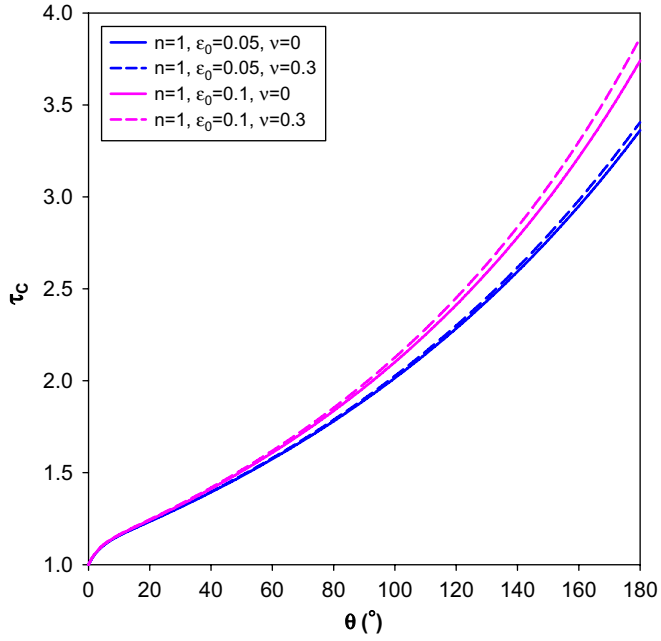

Fig. 10. Apparent tension ratio versus contact angle θ at $v = 0$, and 0.3.

In summary, the effect of Poisson's ratio also increases the tension ratio. But the amount is almost negligible since the reduction of the rod radius due to Poisson's effect is at most 7.8%. Average strain throughout the rod is up to 2.6 times larger than the initial strain. But this contribution leads to at most 1.078 times larger radius ratio than the initial rod radius. Thus, it is well enough to consider the extensibility effect on the increase of the tension ratio.

4. Conclusions

We have established a revised capstan model by adding both extensibility and the Poisson effect of the rod, along with the bending rigidity and nonlinear friction, and solved it numerically. From the present analysis, the following conclusions have been drawn:

1. The rod extensibility enhances the tension ratio competing with the reversing effects of rod rigidity and frictional nonlinearity. In case of linear frictional behavior, larger initial strain renders more increase of the tension ratio. This effect becomes more remarkable at high radius ratio and low modulus. However, the effect of frictional power–law may oppress the effect of rod extensibility since the increase of the initial strain causes the increase of the initial tension, and the larger initial tension decreases the tension ratio more.
2. The effect of Poisson's ratio also increases the tension ratio. Calculated average strain throughout the rod was up to 2.6 times larger than initial strain. But the amount is almost negligible since the reduction of the rod radius due to Poisson's effect is at most 7.8%. The contribution of Poisson's ratio ($v = 0.3$) to the tension ratio is equivalent to the contribution of 1.078 times larger radius ratio at most. Thus, it is well enough to consider the extensibility effect only.
3. The initial tension plays an important role once the modification of the Amonton's law of friction into power–law relationship is applied. Power–law frictional relationship ($n = 0.67$) decreases the tension ratio, but only at the initial tension level sufficiently large. At relatively high initial tension, its effect dominates over all the other factors, while they may compete with it at low initial tension.

We also presented several prerequisites to establish the model. Three major issues about this model were introduced and clarified.

Acknowledgments

This work was supported by the Korea Research Foundation Grant funded by the Korean Government (MOEHRD, KRF-2005-214-D000407), and National Textile Center (NTC) in University of California at Davis. This work was also partially supported by the SRC/ERC Program of MOST/KOSEF (R11-2005-065) through the Intelligent Textile System Research Center (iTRC) at Seoul National University.

References

[1] Morton WE, Hearle JWS. Physical properties of textile fibres. 2nd ed. London: Heinemann; 1975. 611p.

[2] Manning TW. Rescue system mechanics. Interim Report, Research Report to Mountain Rescue Association, 〈http://www.this.net/~frank/pstill.html〉; 2000.
[3] Attaway SW. The mechanics of friction in rope rescue. in: International Technical Rescue Symposium, 1999.
[4] Tu CF, Fort T. Study of fiber-capstan friction. 1. Stibeck curves. Tribol Int 2004;37:701–10.
[5] Tu CF, Fort T. A study of fiber-capstan friction. 2. Stick-strip phoenomena. Tribol Int 2004;37:711–9.
[6] Budinski KG. Friction of plastic webs. Tribol Int 2001;34:625–33.
[7] Greenwood K. The friction twisting of continuous filament yarns. Tribol Int 1985;18(3):157–63.
[8] Werkmeister J, Slocum A. Theoretical and experimental determination of capstan drive stiffness. Precision Engineering 2007;31(1):55–67.
[9] Stuart JM. Capstan equation for strings with rigidity. Br J Appl Phys 1961;12:559–62.
[10] Martin AJP, Mittelmann R. Some measurements of the friction of wool and mohair. J Textile Inst 1946:T269–80.
[11] Howell HG. The general case of friction of a string round a cylinder. J Textile Inst 1953;44(8):T359–62.
[12] Howell HG. The friction of a fiber round a cylinder and its dependence upon cylinder radius. J Textile Inst 1954;45(8):T359–62.
[13] Wei M, Chen R. An improved capstan equation for nonflexible fibers and yarns. Textile Res J 1998;68(7):487–92.
[14] Jung JH, Kang TJ, Youn JR. Effect of bending rigidity on the capstan equation. Textile Res J 2004;74(12):1085–96.
[15] Jung JH, Pan N, Kang TJ. Tension transmission via an elastic rod gripped by two circular-edged plates. Int J Mech Sci 2007;49:1095–103.
[16] Jung JH, Pan N, Kang TJ. Capstan equation including bending rigidity and non-linear frictional behavior. Mech Mach Theory 2008, in press, doi:10.1016/j.mechmachtheory.2007.06.002.